Journal of Non-Crystalline Solids 505 (2019) 115–121

Contents lists available at ScienceDirect

Journal of Non-Crystalline Solids

journal homepage: www.elsevier.com/locate/jnoncrysol

Raman and photoluminescence studies of europium doped zinc-fluorophosphate glasses for photonic applications

V.B. Sreedhar[a,b], K. Venkata Krishnaiah[b], S.K. Nayab Rasool[b], V. Venkatramu[c], C.K. Jayasankar[a,*]

[a] Department of Physics, Sri Venkateswara University, Tirupati 517501, India
[b] Department of Physics, R.G.M. College of Engineering and Technology, Nandyal 518501, India
[c] Department of Physics, Yogi Vemana University, Kadapa 516005, India

ARTICLE INFO

Keywords:
Europium
Zinc-fluorophosphate glasses
Electron-phonon coupling strength
Judd-Ofelt parameters
Radiative properties

ABSTRACT

Europium (Eu^{3+})-doped zinc-fluorophosphate (PKAZfEu) glasses have been synthesized by usual melt-quenching technique. Optical absorption, photoluminescence excitation, photoluminescence and decay curves of these glasses were measured at room temperature and investigated. The Judd-Ofelt (JO) parameters (Ω_λ, $\lambda = 2$ and 4) were determined from the measured emission spectra and used for quantifying the radiative parameters that include radiative transition probability (A_R), radiative lifetime (τ_R), branching ratios (β_R), effective bandwidths ($\Delta\lambda_{eff}$) and peak stimulated emission cross-section ($\sigma(\lambda_P)$) for the $^5D_0$ luminescent state of Eu^{3+}. The electron-phonon coupling strength and phonon energy of the glasses were obtained from the phonon sideband spectrum. The chromaticity coordinates for different concentration of PKAZfEu glasses were evaluated by analyzing the emission spectra with Commission International de l'Eclairage (CIE) color diagram. Decay curves of Eu^{3+} ions for the $^5D_0 \rightarrow {}^7F_2$ transition have been obtained under 393 nm excitation. The decay curves exhibit a single exponential behavior for all the investigated glasses. Luminescence properties of Eu^{3+} ion for the $^5D_O \rightarrow {}^7F_2$ transition indicate that the PKAZfEu glasses could be a suitable gain medium for visible red lasers and display devices.

1. Introduction

Development of novel lanthanide (Ln^{3+})-doped luminescent materials for photonic devices have drawn significant interest in the scientific and technological point of view [1–4]. These Ln^{3+}-doped luminescent materials can find applications in diverse fields of photonics such as optical data storage, remote sensors, upconversion lasers, color displays, infrared laser viewers, indicators, optical printing, etc. Now-a-days, phosphate glasses were also investigated due to their immense potential for bio-applications. However, these glasses alone do not have much chemical durability compared to multi component-phosphate glasses. These glasses modified with sodium, calcium, magnesium, and zinc were established abundance of interest.

Moreover, fluorophosphate glasses exhibit the combined advantages of fluoride and oxide matrices including good moisture resistance, relatively low refractive index, extended transparency from near ultraviolet (UV) to mid infrared (MIR) range, relatively low phonon energy, therefore, these are the suitable hosts for Ln^{3+} ions [5,6]. However, ZnO plays a role of distribution of Ln^{3+} ions through the matrix to prevent non-radiative relaxations which leads to enhance the fluorescent emission [7]. It is challenging to reduce OH^- groups in phosphate glasses, however, these can be minimized significantly in fluorophosphate glasses without the use of control atmosphere for making the glass. Further, with the addition of zincfluoride content to the glass matrix, which minimize the OH^- groups and hence increases the radiative emission of the fluorescent level [8]. In the present host, Al_2O_3 is introduced to the phosphate glasses to expand their mechanical properties.

Usually, most of the Ln ions present a single valence state in glasses, i.e. 3+ state, while europium exhibit both valence states, 2+ and 3+. Addition of europium (Eu^{3+}) ion in these glasses brings a significant change in their optical, structural and magnetic behavior, which is useful in finding new applications. A detailed structural investigations of these glasses becomes highly essential. These Eu^{3+}-doped glasses are mostly utilized for field emission technology as a red emitting phosphors because of their narrow emission at around 610 nm [9]. The Eu^{3+}-doped glasses got a special attention due to the following reasons.

(i) At room temperature, persistent spectral hole burning has been applied to the $^5D_0 \rightarrow {}^7F_0$ transition of Eu^{3+} as it has a potential

* Corresponding author.
E-mail address: ckjaya@yahoo.com (C.K. Jayasankar).

https://doi.org/10.1016/j.jnoncrysol.2018.10.035
Received 26 July 2018; Received in revised form 22 October 2018; Accepted 23 October 2018

practice for high density optical data storage application [10].

(ii) To estimate the local structure around the Ln ions, Eu^{3+} ion is the most desirable one as its fluorescence is highly sensitive under the effect of environment as well as relatively modest energy level scheme [11].

(iii) Magnetic-dipole transition, $^5D_0 \rightarrow {}^7F_1$ (orange emission) of Eu^{3+} is not influenced significantly by the site symmetry as it is parity allowed transition. On the other hand, the red emission (610–630 nm region) due to electric-dipole transition, $^5D_0 \rightarrow {}^7F_2$ gains in intensity as there is a decrease of symmetry [12].

This paper reports the zinc-fluorophosphate glasses doped with varying Eu^{3+} ion concentration. These glasses have been analyzed through X-ray diffraction (XRD), differential thermal analysis (DTA), Raman, absorption, photoluminescence and decay curves. The glass transition and crystallization temperatures were obtained from the DTA. Raman spectrum is used for identifying the various functional groups of the glass. Luminescence properties of the glass samples were evaluated and compared with reported Eu^{3+}-doped systems.

2. Experimental techniques

2.1. Glass synthesis

The Eu^{3+}-doped zinc-fluorophosphate glasses with the molar composition of $44P_2O_5 + 17K_2O + 9Al_2O_3 + (30-x)\ ZnF_2 + x\ Eu_2O_3$ (where x = 0.01, 0.05, 0.1, 0.5, 1.0, 2.0 and 3.0 mol% labeled as PKAZfEu0.01, PKAZfEu0.05, PKAZfEu0.1, PKAZfEu0.5, PKAZfEu1.0, PKAZfEu2.0 and PKAZfEu3.0, respectively) were synthesized by usual melt-quenching technique. About 20 g of glass composition was grinded carefully in an agate motor and taken in a platinum crucible. The crucible was heated at 1100 °C for 90 min. in an electric furnace. The melt was then casted onto a brass mold and subsequently annealed at 380 °C for 14 h for reducing the thermal strains. Usually, the glass samples were permitted to cool to room temperature and polished for different characterizations.

2.2. Characterizations

Thickness of the glass was assessed by a digital screw gauge. Density of the samples was estimated by the Archimedes' method with de-ionized water as dipping liquid. Abbe refractometer is used for measuring the index of refraction of the glasses at a wavelength of 589.3 nm with1-bromonaphthalene ($C_{10}H_7Br$) as adhesive liquid. Physical properties of the glasses were evaluated from the values of thickness, index of refraction, density and concentration using relevant expressions [13,14] and presented in Table 1. The experiments have been repeated to estimate errors. Therefore, all the above properties were measured for three times and are further used to compute mean and standard deviation using the expression [15].

Standard deviation (σ) $= \sqrt{\frac{\sum(x-y)^2}{N.}}$

where x is the actual measurement reading, y is the mean reading and N is the number of measurements.

Table 1
Physical and optical properties of Eu^{3+}: PKAZfEu1.0 glass.

Refractive index, n	1.55 (± 0.01)
Density, d (gm/cc)	3.149 (± 0.002 g/cc)
Optical path length, l (mm)	1.72 (± 0.01 mm)
Concentration, C (10^{20} ions/c.c)	3.126 (± 0.002 ions/cc)
Inter nuclear distance, r_i (Å)	14.73 (± 0.001 A°)
Dielectric constant, ε	2.403 (± 0.021)
Reflection losses, R (%)	4.652 (± 2%)
Molecular refractivity, R_m (cc)	12.28 (± 0.03)
Molecular electron polarization factor, α	2.44×10^{-22}
Polaron radius, r_p (Å)	5.9 (± 0.01A°)

The XRD profile of the glass was obtained using the X-ray diffractometer (RIGAKU; Miniflex-600) under CuKα1 (1.5406 Å) rays excitation. Thermal behavior of the glasses was obtained in the temperature range of 30–1300 °C using DTA (Model: Exstar TG/DTA 6300). About 11.30 mg of the glass sample in the form of powder was taken in an alumina pan of DTA setup and was then examined at the heating rate of 5 °C/min under nitrogen atmosphere with a flow rate of 200 ml/min.

Raman spectrum of the glass sample was recorded by using Raman spectrometer (Lab Ram HR800) under the wavelength of 514 nm (Ar^+ laser) excitation and the signal was collected under the geometry of back scattering. The absorption spectrum of glass sample was measured by using JASCO UV (V-670) spectrophotometer in the wavelength range of 200–2300 nm. The JOBIN YVON fluorolog–3 spectrofluorometer with xenon lamp an excitation source has been used for measuring the photoluminescence, photoluminescence excitation and decay profiles.

3. Results and discussion

3.1. X-ray diffraction spectrum

The X-ray diffraction (XRD) technique is used to recognize the structure of the materials. XRD profile of PKAZfEu1.0 glass is shown in the Fig. 1 that displays a broad hump at lower diffraction angles (pronounced structure), confirms the amorphous nature of the PKAZfEu1.0 glass.

3.2. Differential thermal analysis

Differential thermal analysis (DTA) profile of PKAZfEu1.0 glass is shown in Fig. 2. Thermal analysis explores the glass transition (T_g, 638 °C, ± 2/°C), crystallization (T_c, 926 °C, ± 2/°C) and melting (T_m, 1100 °C, ± 2/°C) temperatures of the PKAZfEu1.0 glass. The factor of glass stability ($\Delta T = T_x - T_g$) and the Hruby's parameter (H) of PKAZfEu1.0 glass were found to be 288 °C and 1.65, respectively. The high value of ΔT = 288 °C, ± 2/°C, evidences that the present glass found to be suitable as a potential candidate for fiber drawing ability. A large value of T_g is essential to reduce the thermal damage of the sample which can be used in high power lasers [16,17]. Glass with relative stability and durability could be designated for laser applications.

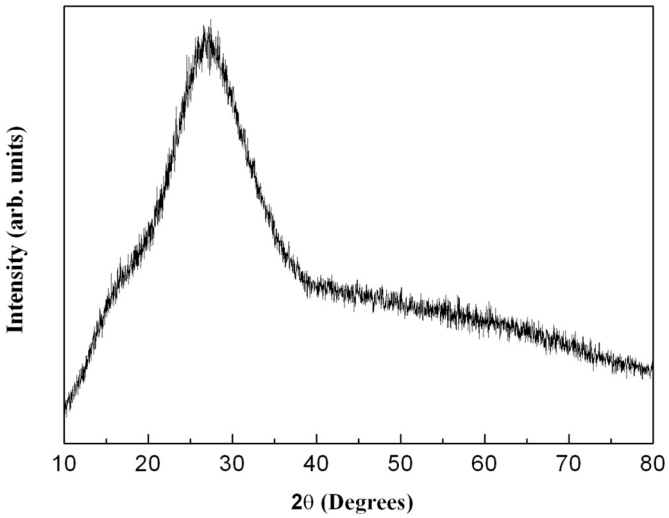

Fig. 1. XRD pattern of PKAZfEu1.0 glass.

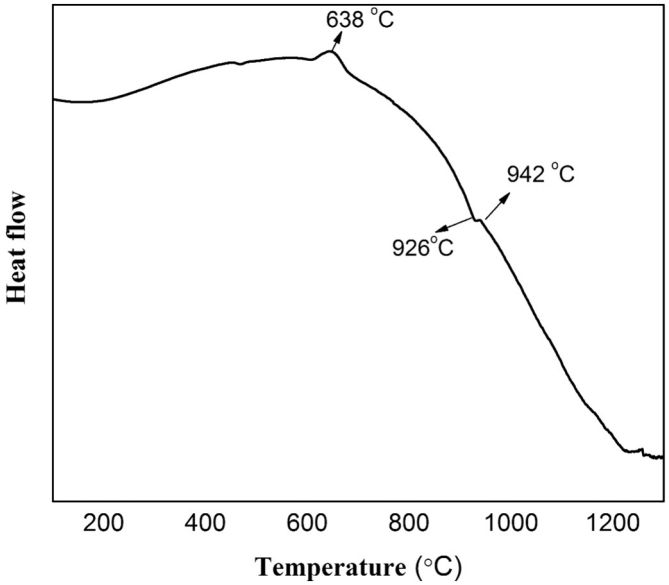

Fig. 2. Differential thermal profile of PKAZfEu1.0 glass.

3.3. Raman spectrum

Raman spectrum of PKAZfEu1.0 glass is shown in Fig. 3, reveals seven characteristic bands at 358, 530, 637, 755, 930, 1091 and 1144 cm^{-1} that are associated to the vibrations of phosphate groups [18]. Raman modes of the phosphate glass network can be analyzed in the spectral regions including modes of non-bridging oxygen (~905–1140 cm^{-1}), bridging oxygen (~700–900 cm^{-1}) and deformation (~500 cm^{-1}).

Usually, phosphate network is developed from the corner sharing of tetrahedral units of PO_4 [19]. The band centered at 1144 cm^{-1} relates the symmetric stretching vibration of O-P-O groups in the Q^1 tetrahedra of metaphosphate glass [20,21]. Band centered at 1091 cm^{-1} governs the mode of asymmetric stretching of P-O-P groups that are linked with metaphosphate groups [22–24]. A band positioned at 930 cm^{-1} relates the mode of P—O symmetric stretching vibrations (it relates to the non-bridging oxygens on the Q^0 tetrahedral groups). The reason to increase Q^0 groups might be due to the rupture of phosphate chains [25]. Raman band at 755 $cm^{-1}$is related to the symmetric stretching vibrational mode of P—O—P bridging bond in Q^1 structure [26–29]. This indicates further rupture of phosphate groups. The weak band positioned at 637 cm^{-1} belongs to the vibration modes of Al_2O_3 [18,30]. A band centered at 530 cm^{-1} corresponds to twisting vibrations of O—P—O and PO_2 modes. Raman band at 358 cm^{-1} relays about the skeletal deformation vibrations of various phosphate chains and PO_3 deformation [31,32]. From the Raman analysis, phonon energy of PKAZfEu1.0 is found to be 1144 cm^{-1} that plays a vital character on the photoluminescence properties of Eu^{3+} ions.

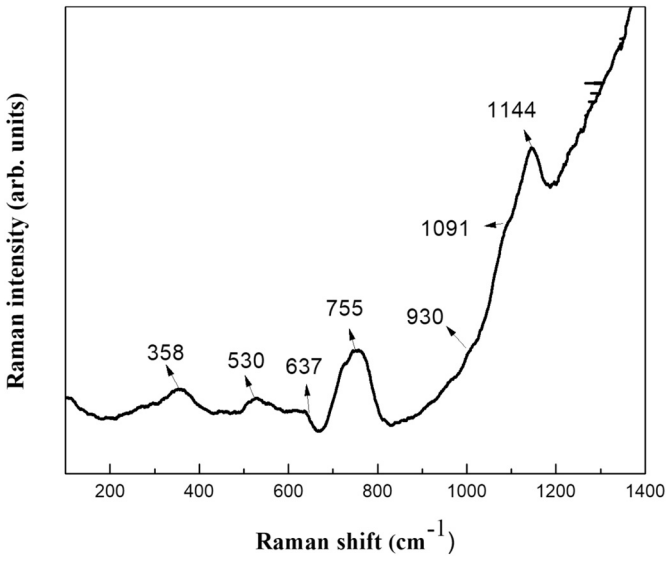

Fig. 3. Raman spectrum of PKAZfEu1.0 glass.

3.4. Optical absorption and excitation spectra

Fig. 4. (a) and (b) displays the optical absorption profile of 1.0 mol% Eu_2O_3-doped zinc-fluorophosphate glass in the UV-visible and NIR regions. These bands are ascribed due to a typical $4f^6$ – $4f^6$ optical transition of Eu^{3+} ions from both the ground ($^7F_0$) and excited ($^7F_1$) states. Absorption bands in the UV-visible region are centered at 362, 376, 382, 393, 465, and 525 nm are ascribed to the $^7F_0 \rightarrow {}^5D_4$, $^5G_3$, $^5G_2$, $^5L_6$, $^5D_2$, and $^5D_1$ transitions, respectively. In addition, some of the transitions centered at 413 and 535 nm are assigned to $^7F_1 \rightarrow {}^5D_3$ and $^5D_1$. Absorption bands in NIR region are correspond to $^7F_0 \rightarrow {}^7F_6$ (2087 nm) and $^7F_1 \rightarrow {}^7F_6$ (2208 nm) transitions. The absorption transition, $^7F_0 \rightarrow {}^5L_6$ is more intense although it do not followed by the selection rules (ΔS and ΔL), however it is followed by ΔJ rule. The $^7F_0 \rightarrow {}^5D_2$ transition is allowed transition of induced electric-dipole and it is hypersensitive to the environment about the Eu^{3+} ions and the $^7F_0 \rightarrow {}^5D_1$ transition is allowed transition of magnetic-dipole.

The photoluminescence (PL) excitation spectrum of PKAZfEu1.0 glass was obtained by screening a red emission at 610 nm is shown in Fig. 5. The spectrum comprises of characteristic excitation bands of Eu^{3+} ion centered at 362 nm (27,624 cm^{-1}, $^7F_0 \rightarrow {}^5D_4$), 376 nm (26,595 cm^{-1}, $^7F_0 \rightarrow {}^5G_3$), 382 nm (26,178 cm^{-1}, $^7F_0 \rightarrow {}^5G_2$), 394 nm (25,380 cm^{-1}, $^7F_0 \rightarrow {}^5L_6$), 415 nm (24,096 cm^{-1}, $^7F_1 \rightarrow {}^5D_3$), 465 nm (21,505 cm^{-1}, $^7F_1 \rightarrow {}^5D_2$), 526 nm (19,011 cm^{-1}, $^7F_0 \rightarrow {}^5D_1$) and 534 nm (18,726 cm^{-1}, $^7F_1 \rightarrow {}^5D_1$). More intense absorption bands are observed in the excitation spectrum that is centered at 394 nm and 465 nm corresponds to the $^7F_0 \rightarrow {}^5L_6$ and $^7F_0 \rightarrow {}^5D_2$ transitions. It is remarkable that the excitation bands in the wavelength range of 380–480 nm, are much stronger for utilizing these glasses for different device applications.

3.5. Fluorescence spectra and Judd-Ofelt analysis

Emission spectra of PKAZfEu glasses are shown in Fig. 6. The spectra display five bands centered at 579 nm (17,271 cm^{-1}, $^5D_0 \rightarrow {}^7F_0$), 585 nm (17,094 cm^{-1}, $^5D_0 \rightarrow {}^7F_1$), 612 nm (16,339 cm^{-1}, $^5D_0 \rightarrow {}^7F_2$), 654 nm (15,290 cm^{-1}, $^5D_0 \rightarrow {}^7F_3$) and 702 nm (13,888 cm^{-1}, $^5D_0 \rightarrow {}^7F_4$). Red emission centered at 610 nm is the strongest among the other transitions. The intensity of emission of the electric-dipole transition, $^5D_0 \rightarrow {}^7F_2$ depends significantly on the native symmetry about the Eu^{3+} ion. On the other hand, the intensity of the magnetic-dipole transition, $^5D_0 \rightarrow {}^7F_1$ is liberated of the native symmetry. It is observed that no significant difference in the profiles and peak positions but their emission intensities increase slightly with increasing Eu^{3+}concentration.

The Judd-Ofelt (JO) parameters, Ω_2 and Ω_4 were determined using the measured emission spectra by considering the intensity ratios of the $^5D_0 \rightarrow {}^7F_{2,4}$ and $^5D_0 \rightarrow {}^7F_1$ transitions. JO intensity parameters follow the tendency as $\Omega_2 > \Omega_4$ and matched to other reported Eu^{3+}: glasses [33–38] as shown in Table 2. However, the Ω_6 parameter is not attained because of the non-appearance of $^5D_0 \rightarrow {}^7F_6$ transition. Consequently, the Ω_6 parameter is considered as zero for evaluating the radiative parameters. The parameter, Ω_2 indicates the nature of the bond (covalent bond) and/or the structural variations in the locality of the Eu^{3+} ions. On the other hand, viscosity and stiffness of the glass can be explained by the parameters, Ω_4 and Ω_6.The asymmetric ratio 'R' (ratio

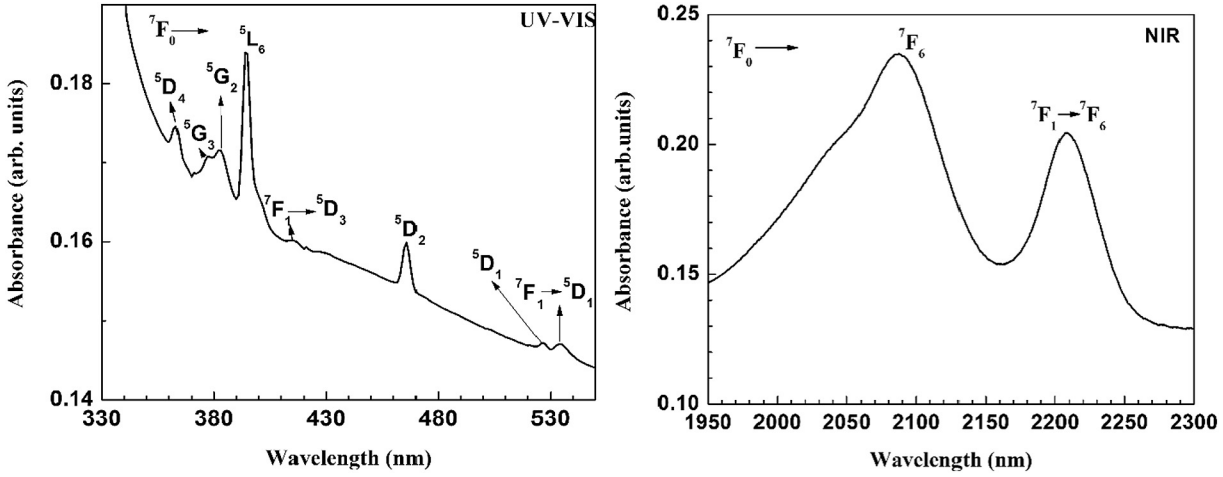

Fig. 4. Optical absorption spectra of PKAZfEu1.0 glass in the UV-Visible and NIR regions.

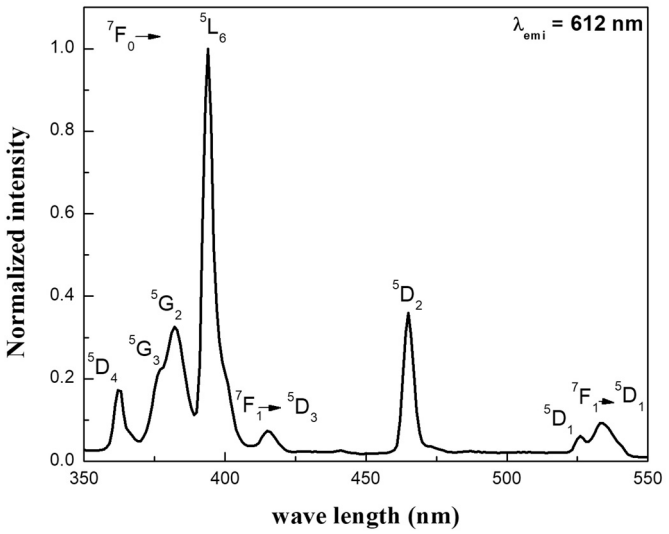

Fig. 5. Excitation spectrum of PKAZfEu1.0 glass.

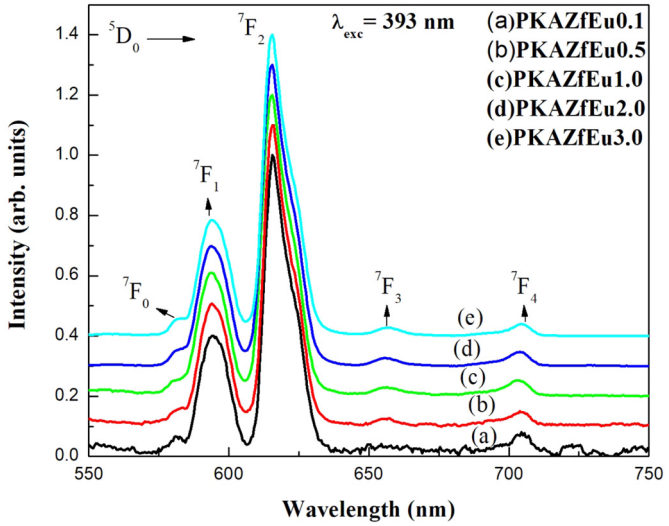

Fig. 6. Luminescence spectra of PKAZfEu glasses. Lines are shifted vertically for better comparison.

between integrated intensities of $^5D_0 \rightarrow {}^7F_2$ and $^5D_0 \rightarrow {}^7F_1$ transition) allows one to estimate the covalent nature around the Eu^{3+} ions and the centro-symmetric modification of Eu^{3+} ion site. As the 'R' value increases, the symmetry about the Eu^{3+} ions decreases and the Eu-O covalency increases and vice versa [39,40]. The value of 'R' is found to be 2.39 which is lower than those of the other reported glasses [33–38] as shown in the Table 2.

Table 3 presents the radiative properties of luminescent levels of Eu^{3+} ion in PKAZfEu1.0 glass that can be determined using JO intensity parameters. From the Table 3, 'A_R' is found to be 128 s^{-1} which is significantly higher in magnitude for the $^5D_0 \rightarrow {}^7F_2$ transition. Both, the derived and experimental branching ratios are comparable to each other for $^5D_0 \rightarrow {}^7F_J$ transitions of Eu^{3+} ion. It is evidenced that any emission transition whose branching ratio is bigger than 0.50, could be suitable for an efficient laser emission [41]. However, the β_{exp} for the $^5D_0 \rightarrow {}^7F_2$ transition is found to be 0.63. Effective bandwidth ($\Delta\lambda_{eff}$) and stimulated emission cross-section ($\sigma(\lambda_p)$) for $^5D_0 \rightarrow {}^7F_J$ (J = 0, 1, 2, 3 and 4) transitions of Eu^{3+} ion were calculated [11,42,43] and presented in Table 3. The $\sigma(\lambda_p)$ is also a significant one which expects the laser emission of the material. The large value of $\sigma(\lambda_p)$ of Eu^{3+} ions for $^5D_0 \rightarrow {}^7F_2$ transition indicates that the PKAZfEu glass is a promising material for the development of optical devices around at 615.5 nm.

3.6. Phonon sideband spectra

Phonon sideband spectroscopy is a suitable technique to explore the local structure around the Ln ions [44]. Absorption bands are due to the interaction of incident photon with the lattice in the form of phonons around the Ln ions [45,46]. Phonon energy (hω) and strength of electron-phonon coupling (g) of the host matrix were estimated, which alter the multi-phonon relaxation processes significantly. The influence of the fluoride component reduces the phonon energy of the glass matrix. Fig. 7 shows the phonon side band (PSB) and pure electronic transition (PET) of the Eu^{3+}:$^7F_0 \rightarrow {}^5D_2$ transition. This PET, $^7F_0 \rightarrow {}^5D_2$ is situated at 465 nm while the PSB (joined to PET) is observed at 441 nm. The contrast between the peak positions of PSB and PET signifies the phonon energy of the glass matrix [44] which was found to be 1171 cm^{-1} for the investigated glass. Phonon energy of the PKAZfEu1.0 glass obtained from both Raman spectrum and PSB spectrum are in good agreement.

In fluorophosphate glasses, interactions are mainly due to the contribution of multi-phonon relaxation and value of 'g' of phonon sideband that connected with the phosphate (PO_2) groups. The 'g' is the comparative amount of PSB line-strength and it can be evaluated by $g = \int I_{PSB} d\upsilon / \int I_{PET} d\upsilon$, where I_{PSB} is the intensity of phonon sideband and I_{PET} is the intensity of the pure electronic transition. The value of 'g' is

Table 2
Glass lables, intensity ratios of $^5D_0 \rightarrow {}^7F_2$ to $^5D_0 \rightarrow {}^7F_1$ (R(2/1)) transitions, Judd-Ofelt parameters (Ω_λ, $\times 10^{-20}$ cm^2), refractive index (n), experimental τ_{exp} (ms) and calculated τ_{cal} (ms) lifetimes and quantum efficiency (η %) for $^5D_0$ level of Eu^{3+}-doped glasses.

Glass lable	R (2/1)	Ω_2	Ω_4	n	τ_{exp}	τ_{rad}	$\eta = \tau_{exp}/\tau_{rad}$
PKAZfEu1.0 [present]	2.39 (± 0.03)	3.73	0.33	1.55 (± 0.02)	2.35 (± 0.04)	5.36 (± 0.10)	43.84 (± 5%)
ZFPEu10 [33]	2.48	3.62	0.41	1.54	2.47	5.55	44.50
NaBE [34]	4.32	5.56	1.85	1.58	2.13	3.23	65.90
PKSAEu [35]	4.43	5.78	0.79	1.524	2.50	3.99	62.65
PKBAEu [36]	4.55	6.91	5.01	–	2.51	2.64	95.00
PKBFAEu [37]	4.69	7.13	5.18	–	2.52	2.60	97.00
PKBAFEu [37]	5.29	8.12	5.79	–	2.46	2.35	105.00
Lithium borate [38]	3.73	6.14	5.04	1.573	1.89	2.68	70.50

found to be 1.4×10^{-2}. The '$\hbar\omega$' and 'g' are compared with the other reported glasses [33,47,48] as shown in Table 4.

3.7. Chromaticity color co-ordinates

To reflect the color of luminescence of the investigated glasses it is essential to represent the color coordinates on the standard chromaticity diagram. The color coordinates have been calculated based on the Commission International deI'Eclairge (CIE) 1931 standard diagram using the emission spectra [49]. CIE 1931 chromaticity coordinates of PKAZfEu glasses under 393 nm excitation are shown in Fig. 8. All the color coordinates of PKAZfEu are located in the intense red region. CIE coordinates are considerably stable with increase of Eu^{3+} ion concentration. Here the chromaticity coordinates are closer to the standard equal energy red light illumination, therefore, they exhibit intense red region in the diagram of chromaticity. Hence, the PKAZfEu glasses could be used as a potential candidate for the red emitting devices applications.

3.8. Decay analysis

Decay curves of Eu^{3+} ion for the $^5D_0$ level as a function of Eu^{3+} concentration under a wavelength of 393 nm excitation by screening the $^5D_0 \rightarrow {}^7F_2$ transition are shown in Fig. 9, which reveal a single exponential behavior. The τ_{exp} of $^5D_0$ level is found to be 2.23, 2.40, 2.59, 2.35, 2.34 and 2.37 ms for PKAZfEu0.05, PKAZfEu0.1, PKAZfEu0.5, PKAZfEu1.0, PKAZfEu2.0 and PKAZfEu3.0 glasses, respectively. The lifetime increased slightly from 0.05 to 0.5 mol% and thereafter decreases slightly from 0.5 to 3.0 mol% concentration. This directs the non-radiative energy transfer process is vanishes among the Eu^{3+} ions. Lifetime of $^5D_0$ level of Eu^{3+} ions in the PKAZfEu glasses is shown in Table 2 and it is matched with those of other reported Eu^{3+}-doped glasses [33–38]. It is observed that the lifetime is higher than those of NaBE [34] and lithium borate [38] glasses.

4. Conclusions

Spectroscopic features of Eu^{3+}-doped zinc-fluorophosphate glasses were investigated as a function of Eu^{3+} concentration. The JO parameters were derived for PKAZfEu1.0 glass from the emission spectrum. A high value of Ω_2 intensity parameter reflects that the Eu^{3+} ions situated at a highly polarized environment. Radiative parameters of the emitting level, $^5D_0$ of Eu^{3+} ions were evaluated by using the Judd-Ofelt parameters. The color coordinates of Eu^{3+}-doped glasses appear within the red light region. Photoluminescence intensity of Eu^{3+} ions increased with increasing concentration and no concentration quenching was witnessed for the range of concentrations. Decay curves of $^5D_0$ level of Eu^{3+} unveil a mono-exponential nature for the investigated samples.

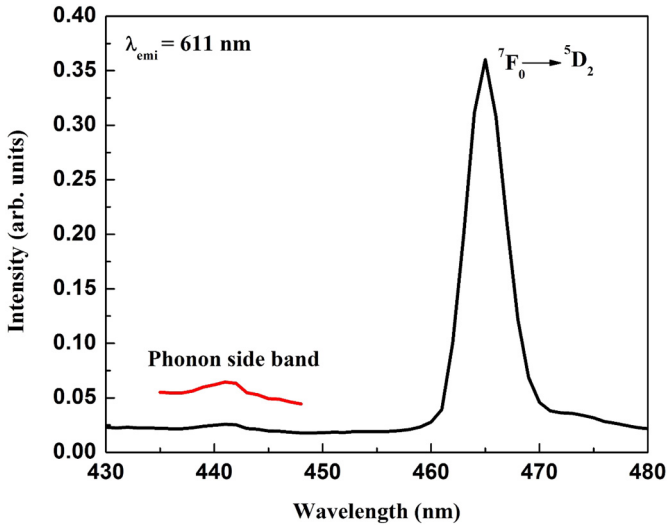

Fig. 7. Phonon side band (PSB) and pure electronic transition (PET) of PKAZfEu1.0 glass.

Table 4
Comparison of phonon energy ($\hbar\omega$, cm^{-1}) and coupling strength (g) of Eu^{3+}: glasses.

Glass	$\hbar\omega$ (cm^{-1})	g (10^{-2})
PKAZfEu1.0 [Present glass]	1171	1.4
ZFPEu10 [33]	1130	2.4
Lithium fluoroborate [47]	1675	2.1
Phosphate [48]	1200–1350	1.2
Borate [48]	1340–1480	1.8
Fluoride [48]	500–600	1500–3500

Table 3
Emission band positions (λ_p, nm), effective band widths ($\Delta\lambda_{eff}$, nm), radiative transition probability (A_R, s^{-1}), peak stimulated emission cross-section ($\sigma(\lambda p)$, $\times 10^{-22}$ cm^2), experimental and calculated branching ratios (β_R) for $^5D_0$ level of Eu^{3+}:PKAZfEu glasses.

Transition $^5D_0 \rightarrow$	λ_p (± 1)	$\Delta\lambda_{eff}$ (± 0.01)	A_R	$\sigma(\lambda_p)$ (± 0.01)	$(\beta_R)_{exp}$ (± 0.0002)	$(\beta_R)_{cal}$
$^7F_0$	581.5	4.86	0.0 (± 0.0)	0.00	0.0234	0.00
$^7F_1$	594	12.35	53.0 (± 0.1)	2.95	0.2630	0.285
$^7F_2$	615.5	12.23	128.0 (± 1.0)	8.27	0.6300	0.68
$^7F_3$	655.5	8.432	0.0 (± 0.0)	0.00	0.0157	0.00
$^7F_4$	703.5	8.918	6.0 (± 0.1)	0.858	0.0300	0.0304

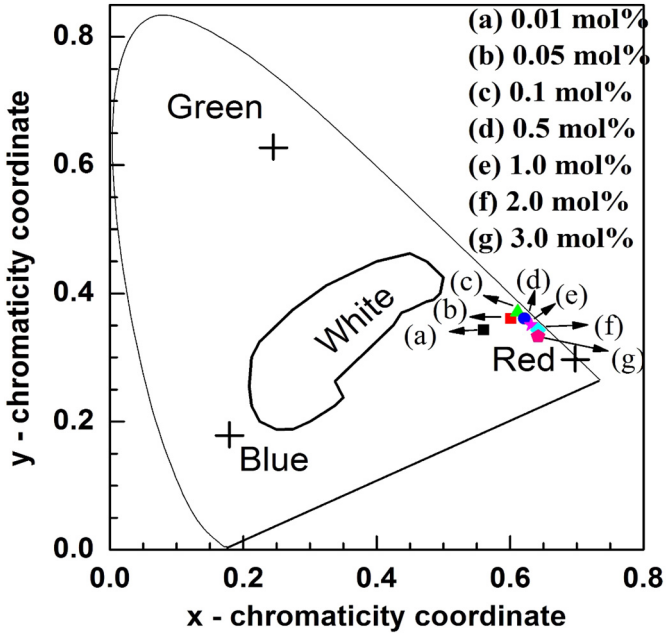

Fig. 8. CIE color coordinates of PKAZfEu glasses with different Eu_2O_3 concentrations.

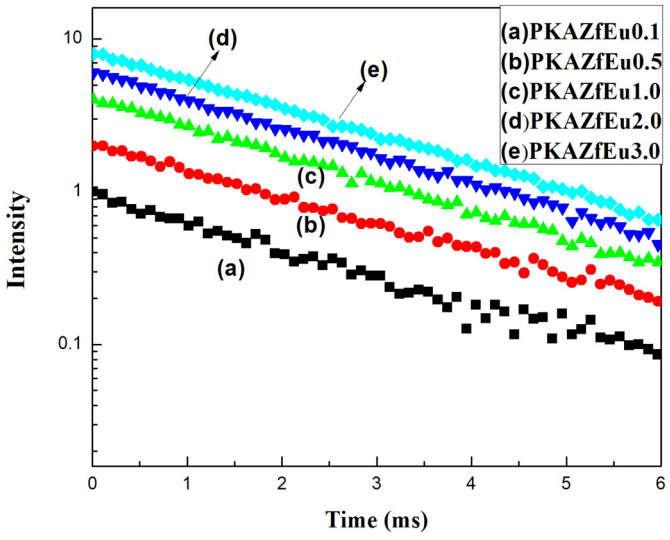

Fig. 9. Fluorescence decay curves of the $^5D_0$ level of Eu^{3+} ions in PKAZfEu glasses. Lines are shifted vertically for better comparison.

A slight variation in the lifetime of the $^5D_0$ level with increasing Eu^{3+} concentration which signifies the non-existence of energy transfer among the Eu^{3+} ions. The results reveal that the present zinc-fluorophosphate glasses could be an appropriate candidate for visible optical device applications.

Acknowledgements

One of the authors (CKJ) is grateful to DAE-BRNS, Govt. of India for the award of research project (No.2009/34/36/BRNS/3174) under MoU between Sri Venkateswara University, Tirupati, RRCAT, Indore and BARC, Mumbai. Dr. KVK is thankful to SERB-DST, Govt. of India, New Delhi for the award of a major research project (File No: EMR/2017/000009).

References

[1] L. Zhu, C. Zuo, Z. Luo, A. Lu, Photoluminiscence of Dy^{3+} and Sm^{3+}: SiO_2-Al_2O_3-LiF-CaF_2 glasses, Physica B 405 (2010) 4401–4406.
[2] E. Malchukova, B. Brizot, D. Ghaleb, G. Petite, Optical properties of pristine and γ-irradiated Sm doped borosilicate glasses, Nucl. Inst. Methods Phys. Res. A A537 (2005) 411–414.
[3] J. Hao, J. Gao, M. Cocivera, Green, blue and yellow cathode luminescence of $Ba_2B_5O_9Cl$ Thin-films doped with Tb^{3+}, Tm^{3+} and Mn^{2+}, Appl. Phys. Lett. 82 (2003) 2224–2226.
[4] P.E.A. Mobert, E. Heumann, G. Huber, B.H.J. Chai, 540 mW of blue output power at 425 nm generated by intracavity frequency doubling an upconversion-pumped Er^{3+}:$YLiF_4$ laser, Appl. Phys. Lett. 73 (1998) 139–141.
[5] L. Zhang, L. Wen, H. Sun, J. Zhang, L. Hu, Influence of TeO_2, PbF_2, ZnF_2 on spectroscopic and lasing properties of Yb^{3+} doped fluorophosphate glasses, J. Alloys Compd. 391 (2005) 156–161.
[6] R. Praveena, R. Vijaya, C.K. Jayasankar, Photoluminiscence and energy transfer studies of Dy^{3+} doped fluorophosphate glasses, Spectrochim. Acta A 70 (2008) 577–586.
[7] S.M. Hsu, S.W. Yung, Y.C. Hsu, F.B. Wu, C. Fu, Y.S. Lai, Y.M. Lee, Enhancement of luminescence properties and the role of ZnO in Tb^{3+} ions doped zinc aluminum phosphate glasses, Ceram. Int. 42 (2016) 4019–4025.
[8] M. Liao, Z. Chao Duan, L. Hu, Y. Fang, L. Wen, Spectroscopic properties of Er^{3+}/Yb^{3+} co-doped fluorophosphate glasses, J. Lumin. 126 (2007) 139–144.
[9] J.K. Krebs, J.M. Brownstein, Site-selective spectroscopy of Eu^{3+} in bioactive glass, J. Lumin. 124 (2007) 257–259.
[10] W.J. Chung, J. Heo, Room temperature persistent spectral hole burning in X-ray irradiated Eu^{3+} − doped Borate Glasses, Appl. Phys. Lett. 79 (2001) 326–328.
[11] V. Lavin, U.R. Rodriguez-Mendoza, I.R. Martin, V.D. Rodriguez, Optical spectroscopy analysis of the Eu^{3+} ions local structure in calcium diborate glasses, J. Non-Cryst. Solids 319 (2003) 200–216.
[12] A. Zhang, M. Lu, G. Zhou, Y. Zhou, Z. Qiu, Q. Ma, Synthesis, characterization and luminescence of Eu^{3+}-doped $SrZrO_3$nanocrystals, J. Alloys Compd. 468 (2009) L17–L20.
[13] V.N. Bykov, A.A. Osipov, V.N. Anfilogov, High-Temperature//Rasplavy, 4 (1997), pp. 28–31.
[14] M. Dejneka, E. Snitzer, R.E. Riman, Blue, green and red fluorescence and energy transfer of Eu^{3+} in fluoride glasses, J. Lumin. 65 (1995) 227–245.
[15] R. Philip Bevington, Data Reduction and Error Analysis for the Physical Sciences, McGraw Hill, 1969.
[16] X. Feng, S. Tanabe, T. Hanada, Spectroscopic properties and thermal stability of Er^{3+} − doped germanotellurite glasses for broad band fiber amplifiers, J. Am. Ceram. Soc. 84 (2001) 165–171.
[17] M. Saad, M. Poulain, Glass forming ability criterion, Mater. Sci. Forum 19 (1987) 8–11.
[18] J.J. Videau, J. Portier, B. Piriou, Raman spectroscopic studies of fluorophosphates glasses, J. Non-Cryst. Solids 48 (1982) 385–392.
[19] J.R. Van Wazer, Phosphorous and Its Compounds, 1 Interscience, NewYork, 1958.
[20] G.B. Rouse, P.J. Miller, W.M. Risen, Mixed alkali glass spectra and structure, J. Non-Cryst. Solids 28 (1978) 193–207.
[21] B.N. Nelson, G.J. Exarhos, Vibrational spectroscopy of cation-site interactions in Phosphate glasses, J. Chem. Phys. 71 (1979) 2739–2747.
[22] L. Koudelka, J. Klikorka, M. Frumar, M. Pisarcik, V. Kello, V.D. Khaleliv, V.I. Vakrameer, G.D. Chkhenkelli, Raman spectra and structure of flurophosphate glasses of (1-*x*)$Ba(PO_3)_2$- *x*$LiRAlF_6$, J. Non-Cryst. Solids 85 (1986) 204–210.
[23] F.H. Elbatal, A.M. Abdelghany, R.L. Elwan, Structural characterization of gamma irradiated lithium phosphate glasses containing various amounts of molybdenum, J. Mol. Struct. 1000 (2011) 103–108.
[24] C. Ivascu, A. Timor Gabor, O. Cozar, L. Doraban, I. Ardelean, FT-IR, Raman and thermo-luminescence investigations of P_2O_5-BaO-Li_2O glass system, J. Mol. Struct. 993 (2011) 249–253.
[25] O. Cozar, D.A. Magdas, L. Nasdala, I. Ardelean, G. Damian, Raman spectroscopic studies of some lead phosphate glasses with tungsten ions, J. Non-Cryst. Solids 352 (2006) 3121–3125.
[26] C.W. Kim, C.S. Ray, D. Zhu, D.E. Day, D. Gombert, A. Aloy, A. Mogus-Milankovic, M. Karabulut, Chemically durable iron phosphate glasses for vitrifying sodium bearing waste (SBW) using conventional and cold crucible induction melting (CCIM) techniques, J. Nucl. Mater. 322 (2003) 152–164.
[27] M. Karabulut, G.K. Marasinghe, C.S. Ray, D.E. Day, O. Oztruk, G.D. Waddill, X-ray photoelectron and Mossbauer spectroscopic studies of iron phosphate glasses containing U, Cs, and B, J. Non-Cryst. Solids 249 (1999) 106–116.
[28] C.W. Kim, D.E. Day, Immobilization of Hanford Law in iron phosphate glasses, J. Non-Cryst. Solids 331 (2003) 20–31.
[29] T. Jermoumi, N. Musthaphahafid, N. Niegisch, M. Mennig, A. Sabir, N. Toreis, Properties of(0.5-*x*)Zn-*x*Fe_2O_3-0.5P_2O_5 glasses, Mater. Res. Bull. 37 (2002) 49–57.
[30] F.X. Gan, Optical and Spectroscopic Properties of Glass, Springer, Berlin/Heidelberg, 1992 (P. 27).
[31] J. Koo, B.S. Bae, H. Na, Raman spectroscopy of copper phosphate glasses, J. Non-Cryst. Solids 212 (1997) 173–179.
[32] K. Meyer, Characterization of the structure of binary zinc ultraphosphate glasses by infrared and Raman spectroscopy, J. Non-Cryst. Solids 209 (1997) 227–231.
[33] N. Vijaya, C.K. Jayasankar, Structural and spectroscopic properties of Eu^{3+}-doped zinc fluorophosphate glasses, J. Mol. Struct. 1036 (2012) 42–50.
[34] K. Marimuthu, S. Surendra Babu, G. Muralidharan, S. Armugam, C.K. Jayasankar, Structural and optical studies of Eu^{3+} ions in alkali borate glasses, Phys. Status.

Solidi. A 206 (2009) 131–139.
[35] K. Linganna, C.K. Jayasankar, Optical properties of Eu^{3+} ions in phosphate glasses, Spectrochim. Acta A 97 (2012) 788–797.
[36] S. Surendra Babu, P. Babu, C.K. Jayasankar, W. Sievers, Th. Troster, G. Wortmann, Optical absorption and photoluminiscence studies of Eu^{3+} doped phosphate and fluorophosphate glasses, J. Lumin. 126 (2007) 109–120.
[37] R. Balakrishnaiah, R. Vijaya, P. Babu, C.K. Jayasankar, M.L.P. Reddy, Charecterization of Eu^{3+} doped fluorophosphate glasses for red emission, J. Non-Cryst. Solids 353 (2007) 1397–1401.
[38] P. Babu, C.K. Jayasankar, Optical spectroscopy of Eu^{3+} ions in lithium borate and lithiumfluoroborate glasses, Physica B 279 (2000) 262–281.
[39] Y. Dwivedi, S.B. Rai, Optical properties of Eu^{3+} in oxyfluoroborate glassand its nano crystalline glass, Opt. Mater. 31 (2008) 87–93.
[40] K. Upendra Kumar, S. Surendra Babu, Ch. Srinivasa Rao, C.K. Jayasankar, Optical and fluoroscence spectroscopy of Eu_2O_3 doped P_2O_5-K_2O-KF-MO-Al_2O_3 (M = Mg, Sr and Ba) glasses, Opt. Commun. 284 (2011) 2909–2914.
[41] J.L. Adam, W.A. Sibley, Optical transitions of Pr^{3+} ions in fluorozirconate glasses, J. Non-Cryst. Solids 76 (1985) 267–279.
[42] B.R. Judd, Optical absorption intensities of rare earth ions, Phys. Rev. 127 (1962) 750–761.
[43] G.S. Ofelt, Intensities of crystal spectra of rare earth ions, J. Chem. Phys. 37 (1962) 511–520.
[44] S. Tanabe, S. Todoroki, K. Hirao, N. Soga, Phonon sideband of Eu^{3+} in sodium borate glasses, J. Non-Cryst. Solids 122 (1990) 59–65.
[45] Y. Yang, B. Chen, C. Wang, H. Zhang, L. Cheng, J. Sun, Y. Peng, X. Zhang, Investigation on structure and optical properties of Er^{3+}, Eu^{3+} single doped Na_2O-ZnO-B_2O_3-TeO_2 glasses, Opt. Mater. 31 (2008) 445–450.
[46] H. Toratani, T. Izumitani, H. Kuroda, Compositional dependence of non-radiative decay rate in Nd laser glasses, J. Non-Cryst. Solids 52 (1982) 303–313.
[47] S. Arun Kumar, K. Marimuthu, Structural and luminiscence studies on Eu^{3+}: B_2O_3-Li_2O-MO-LiF(M = Ba, Bi_2, Cd, Pb, $Sr_2$and Zn) glasses, J. Lumin. 139 (2013) 6–15.
[48] R. Reisfeld, Radiative and non-radiative transitions of rare earths in inorganic glasses, Struct. Bond. 22 (1975) 123–175.
[49] E. Fred Schubert, Light Emitting Diodes, 2ndedition, Cambridge University Press, 2006.